AGU PUBLICATIONS

Geophysical Research Letters

RESEARCH LETTER
10.1002/2016GL071881

Key Points:
- A biogeochemical model realistically simulates eutrophication-induced acidification in the northern Gulf of Mexico
- The sediments, which are a major source of dissolved inorganic carbon (DIC), cause low pH that is restricted to the bottom boundary layer
- The contribution of river-derived organic matter to DIC production and acidification is small in the river outflow region

Supporting Information:
- Supporting Information S1
- Movie S1
- Figure S1
- Figure S2
- Figure S3
- Figure S4
- Figure S5

Correspondence to:
A. Laurent,
arnaud.laurent@dal.ca

Citation:
Laurent, A., K. Fennel, W.-J. Cai, W.-J. Huang, L. Barbero, and R. Wanninkhof (2017), Eutrophication-induced acidification of coastal waters in the northern Gulf of Mexico: Insights into origin and processes from a coupled physical-biogeochemical model, *Geophys. Res. Lett.*, *44*, 946–956, doi:10.1002/2016GL071881.

Received 9 NOV 2016
Accepted 13 JAN 2017
Accepted article online 19 JAN 2017
Published online 30 JAN 2017

©2017. American Geophysical Union. All Rights Reserved.

Eutrophication-induced acidification of coastal waters in the northern Gulf of Mexico: Insights into origin and processes from a coupled physical-biogeochemical model

Arnaud Laurent[1], Katja Fennel[1], Wei-Jun Cai[2], Wei-Jen Huang[3,2], Leticia Barbero[4,5], and Rik Wanninkhof[4]

[1]Department of Oceanography, Dalhousie University, Halifax, Nova Scotia, Canada, [2]School of Marine Science and Policy, University of Delaware, Newark, Delaware, USA, [3]Department of Oceanography, National Sun Yat-sen University, Kaohsiung, Taiwan, [4]NOAA/AOML, Miami, Florida, USA, [5]CIMAS, University of Miami, Miami, Florida, USA

Abstract Nutrient inputs from the Mississippi/Atchafalaya River system into the northern Gulf of Mexico promote high phytoplankton production and lead to high respiration rates. Respiration coupled with water column stratification results in seasonal summer hypoxia in bottom waters on the shelf. In addition to consuming oxygen, respiration produces carbon dioxide (CO_2), thus lowering the pH and acidifying bottom waters. Here we present a high-resolution biogeochemical model simulating this eutrophication-driven acidification and investigate the dominant underlying processes. The model shows the recurring development of an extended area of acidified bottom waters in summer on the northern Gulf of Mexico shelf that coincides with hypoxic waters. Not reported before, acidified waters are confined to a thin bottom boundary layer where the production of CO_2 by benthic metabolic processes is dominant. Despite a reduced saturation state, acidified waters remain supersaturated with respect to aragonite.

1. Introduction

Human activities have a significant impact on the biogeochemistry of the coastal ocean [*Rabouille et al.*, 2001; *Doney*, 2010; *Levin et al.*, 2015]. Among the multiple stressors that affect coastal ecosystems, excess nutrient load from rivers is a ubiquitous issue in populated areas [*Paerl*, 2006]. High concentrations of river-derived dissolved organic and inorganic nitrogen (DON and DIN) and phosphorus (DOP and DIP) stimulate algal production in the coastal ocean; subsequent decomposition of planktonic biomass in combination with vertical stratification can lead to hypoxia in bottom waters [*Rabouille et al.*, 2008]. Hypoxic conditions ($[O_2] < 62.5\ \mathrm{mmol\,O_2\,m^{-3}}$) can have detrimental effects on benthic organisms that propagate through the food web [*Diaz and Rosenberg*, 1995, 2008; *Rose et al.*, 2009] potentially impacting local fisheries [*Selberg et al.*, 2001; *Breitburg et al.*, 2009; *Langseth et al.*, 2014].

In addition to consuming oxygen, algal decomposition produces dissolved inorganic carbon (DIC) and lowers the pH in bottom waters, especially those waters that are prone to hypoxic conditions [*Cai et al.*, 2011]. This eutrophication-induced acidification is an additional stressor in stratified, river-influenced coastal ecosystems. Anthropogenic CO_2 emissions to the atmosphere will further exacerbate eutrophication-induced acidification by imposing a long-term increase in mean DIC concentrations in the upper ocean. The combined effects of rising atmospheric and river-induced anthropogenic CO_2 on coastal waters with the associated decrease in buffer capacity (increasing Revelle factor) will increase the vulnerability of coastal ecosystems to perturbations [*Cai et al.*, 2011; *Altieri and Gedan*, 2014; *Breitburg et al.*, 2015].

Nutrient loads from the Mississippi/Atchafalaya River system, one of the world's largest river basins, promote high phytoplankton production on the continental shelf of the northern Gulf of Mexico [*Lohrenz et al.*, 1990, 1999]. Decomposition of this organic material contributes to recurring hypoxia [*Rabalais et al.*, 2002a] and eutrophication-induced acidification [*Cai et al.*, 2011] in bottom waters in summer. Acidification is expected to increase throughout the 21st century with increasing atmospheric CO_2 [*Cai et al.*, 2011; *Ren et al.*, 2015]. Furthermore, respiration-induced acidification will have a larger effect on pH in this region because the buffering capacity will be reduced [*Sunda and Cai*, 2012]. While hypoxia in the northern Gulf is a long-standing issue [*Rabalais et al.*, 2002b, 2007] and has received significant attention from various

stakeholders [*Environmental Protection Agency*, 2008], the associated acidification problem is only starting to be recognized.

Management efforts to mitigate the negative impacts of stressors like hypoxia and acidification must rely on sound scientific understanding of the underlying processes. Biogeochemical models are important tools for improving process understanding and allow one to assess the impacts of nutrient load reductions through different scenario simulations. While progress has been made in recent years in the development of models that reproduce hypoxia on the Louisiana Shelf [*Fennel et al*., 2011, 2013; *Laurent et al*., 2012; *Justić and Wang*, 2014; *Laurent and Fennel*, 2014; *Yu et al*., 2015a, 2015b], the associated acidification in the area has not yet been investigated by means of a biogeochemical model.

Building on previous model developments, we present a regional biogeochemical model for the northern Gulf of Mexico that explicitly accounts for physical and biogeochemical processes and environmental conditions controlling dissolved oxygen and inorganic carbon dynamics. We show that the model realistically simulates eutrophication-induced acidification and identify and quantify the key processes responsible for bottom water acidification. While our study is regional, the issue of eutrophication-induced acidification is of global concern. Our results could inform investigations of other river-dominated margins with large nutrient loads, for example, in the East China Sea and Bay of Bengal.

2. Methods

Our biogeochemical model is based on a high-resolution, regional circulation model configured with the Regional Ocean Modeling System [*Haidvogel et al*., 2008]. Setup and validation of the circulation model are described in detail by *Hetland and DiMarco* [2008, 2012]. Satellite-derived attenuation coefficients for shortwave radiation [*Schaeffer et al*., 2011; *Ko et al*., 2016] are used to simulate realistic bottom boundary layer thicknesses in the circulation model [*Fennel et al*., 2016]. The circulation model is coupled with the pelagic N-cycle model of *Fennel et al*. [2006, 2008, 2011] with explicit consideration of carbonate chemistry [*Fennel et al*., 2008] and extended to include DIP [*Laurent et al*., 2012], O_2 [*Fennel et al*., 2013], and river dissolved organic matter (DOM) [*Yu et al*., 2015b]. The model has 15 state variables: phytoplankton, chlorophyll, zooplankton, nitrate, ammonium, DIP, O_2, DIC, total alkalinity, and three detritus pools (small and large detritus, river DOM, each split into nitrogen and carbon). The model equations build on several previous studies (including *Eppley* [1972], *Evans and Parslow* [1985], *Garcia and Gordon* [1992], *Geider et al*. [1996, 1997], and *Soetaert et al*. [1996a, 1996b]) and are provided in the supporting information. Simulated surface chlorophyll concentration and primary production and water column respiration rates were shown to agree well with observations [*Laurent et al*., 2012; *Laurent and Fennel*, 2014; *Yu et al*., 2015b].

In the model DIC is produced by zooplankton respiration, remineralization of detritus, and efflux from the sediment. DIC is taken up during phytoplankton growth, and CO_2 is exchanged with the atmosphere at the sea surface. Air-sea gas exchange is prescribed following *Wanninkhof* [2014], which is similar to other recent air-sea gas exchange relationships [*Ho et al*., 2006, 2011]. Alkalinity is affected by sources and sinks of DIN using the explicit conservative expression of total alkalinity [*Wolf-Gladrow et al*., 2007] (see supporting information). Sediment O_2 consumption (SOC) is parameterized as a function of bottom water temperature derived from the diagenetic model simulations of *Laurent et al*. [2016] such that $SOC = 0.614 \times 2^{T/5.474}$ (T in °C; see supporting information). Organic matter (OM) remineralization in the sediment occurs regardless of whether O_2 is present or not. When O_2 is not available, other electron acceptors are used, which are reoxidized when they get in contact with O_2. Hence, OM mineralization in the model does not depend on O_2 in the overlying bottom water. This assumption is consistent with results from a diagenetic model that includes reduced species produced by anaerobic remineralization [see *Laurent et al*., 2016]. Sediment denitrification is accounted for using an empirically derived relationship between SOC and denitrification as described by *Fennel et al*. [2013]. Efflux of NH_4^+, DIC, and alkalinity from the sediment is proportional to SOC using $NH_4^+ : SOC = 0.036$ mol N $(\text{mol } O_2)^{-1}$ and $DIC : SOC = 0.9475$ mol C $(\text{mol } O_2)^{-1}$. For each mole of NH_4^+ produced within the sediment a mole of alkalinity is produced; thus, we assume $F_{TAlk} = F_{NH_4^+}$ (see supporting information). The removal of fixed nitrogen by denitrification results in an effective alkalinity flux out of the sediment [see *Fennel et al*., 2008]. Our model does not include the effects of sulfate reduction, because this process is negligible in the study region [*Morse and Eldridge*, 2007]. However, surface

sediment may become undersaturated with respect to aragonite due to oxic respiration and oxidation of reduced compounds. This would cause $CaCO_3$ dissolution in the sediment and would generate alkalinity fluxes when bottom waters are close to saturation [*Jahnke et al*., 1997]. Since aragonite saturation is generally much larger than 1 in this system, benthic respiration is assumed to not involve $CaCO_3$ dissolution (no associated alkalinity efflux).

pH is calculated using the carbonic acid dissociation constants of *Mehrbach et al*. [1973] as refit by *Dickson and Millero* [1987] and reported on the total scale. In the analyses presented further below, the effect of each biological process on pH is quantified. For each process we recalculate pH with a new DIC concentration that excludes the DIC produced by this process. We follow the same procedure for alkalinity. The effect of each process on pH, due to a change either in DIC or alkalinity, is calculated as the difference between the original and the recalculated pH. We use this procedure because the effect of DIC or alkalinity production on pH differs depending on local temperature, salinity, and buffer factor.

Atmospheric forcing is prescribed using 3-hourly winds from the National Centers for Environmental Prediction (NCEP) North American Regional Reanalysis [*Mesinger et al*., 2006] and climatological surface heat and freshwater fluxes [*Da Silva et al*., 1994a, 1994b]. Mississippi and Atchafalaya River runoff is prescribed using daily freshwater transport estimates by the U.S. Army Corps of Engineers at Tarbert Landing and Simmesport, respectively. Nutrient, particulate organic matter (POM), and DOM loadings are imposed using monthly flux estimates from the U.S. Geological Survey [*Aulenbach et al*., 2007]. POM and DOM loads are added to the small detritus and the river DOM pools, respectively [*Yu et al*., 2015b]. Freshwater discharge and nutrient loads are shown in supporting information Figure S1. Atmospheric pCO_2 is specified using a time-varying climatology derived from measurements collected in the Mississippi Bight over the period 2003–2012 as $pCO_2^{air}(\ \mu atm) = 380.46 + 9.32 \times \sin(2\pi t + 1.07)$, where $0 < t < 1$ (year fraction). River, initial, and boundary concentrations for DIC and alkalinity are specified using observations from 13 surveys of the Louisiana Shelf between 2004 and 2010, described by *Cai et al*. [2010] and *Huang et al*. [2015]. The biogeochemical model was spun up for 1 year in 2006, which is sufficient to reach a periodic steady state in this system and then run for 3 years starting from 1 January 2007.

For model validation we use surface water pCO_2 observations collected in the northern Gulf and derived air-sea CO_2 fluxes [*Huang et al*., 2015] as well as bottom water observations of temperature, salinity, O_2, DIC, and alkalinity from a shelf-wide survey in August 2007 [*Cai et al*., 2011]. We also use shelf-averaged ($z \leq 50$ m), vertically integrated water column respiration rates computed from the shelf-wide surveys of *Murrell and Lehrter* [2011] by assuming a molar carbon to O_2 ratio of 0.69 [*Anderson and Sarmiento*, 1994]. Observations of release of DIC from the sediment are from *Lehrter et al*. [2012].

3. Results and Discussion

Simulated bottom water pH, O_2, and DIC distributions (Figure 1) agree well with the observations from August 2007 by *Cai et al*. [2011] and indicate high DIC concentrations and low pH in the hypoxic zone (Figure 1). Simulated bottom water alkalinity and aragonite saturation state are also in good agreement with the observations (see supporting information Figure S2). It should be noted that in summer, hydrodynamic instabilities along river plume fronts generate high mesoscale variability on the Louisiana Shelf [*Marta-Almeida et al*., 2013] that translates into uncertainty in terms of the exact timing and location of hypoxia [*Mattern et al*., 2013] and, by inference, high DIC/low pH conditions. Some mismatch between model and observations is therefore expected.

The model also simulates well the observed range and seasonal variation in surface pCO_2 (Figure S3) as well as the spatial distribution of surface pCO_2 in summer 2007 and 2009 (Figure S4). Some of the discrepancies in spatial surface pCO_2 patterns between observations and model arise because sampling was not synoptic (it occurred over 5 and 9 days in 2007 and 2008, respectively) and because of the above mentioned mesoscale variability. The simulated regional sea-air CO_2 fluxes are within one standard deviation of the observations in the different salinity regions (Figure S5), except in spring in the midsalinity range ($17 < S < 25$), perhaps because the model underestimates the influence of primary production on surface water pCO_2 in this salinity range. Uptake of CO_2 by the ocean is simulated in spring in the $25 < S < 33$ salinity range and therefore a spatial shift of high primary production toward higher salinity waters ($S > 25$) may contribute to this

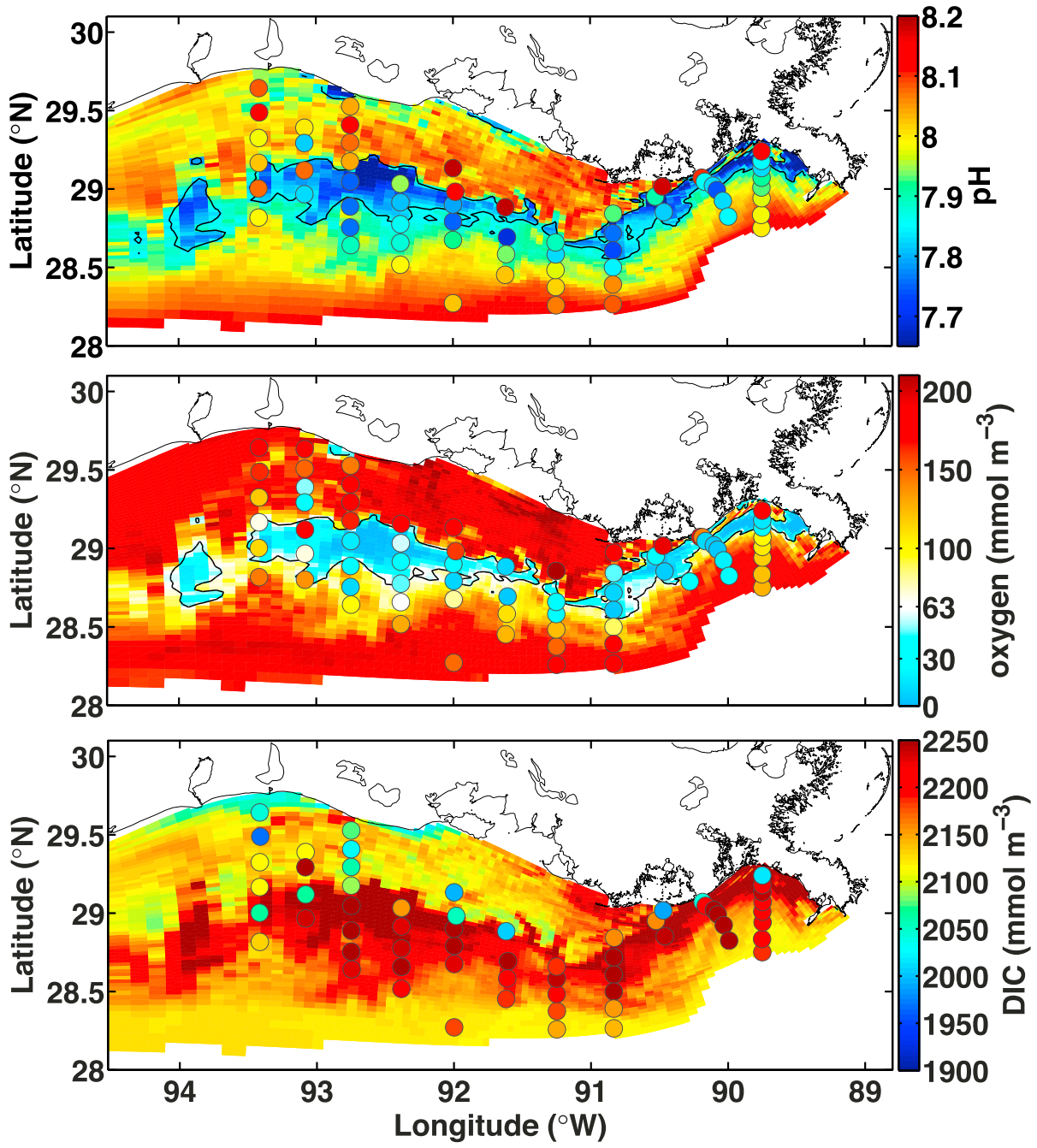

Figure 1. Comparison of simulated bottom water pH, oxygen, and DIC (color maps) on 21 August 2007 with observations (colored circles) from *Cai et al.* [2011] collected over the period 19–24 August 2007.

mismatch. However, since the acidification process we are investigating occurs in summer and in bottom waters, our results should not be unduly affected by the spring mismatch in sea-air CO_2 flux.

3.1. Low pH in Bottom Waters

According to our simulation, bottom water pH varies seasonally and spatially on the northern Gulf of Mexico shelf as follows: in winter, when stratification is relatively weak, bottom water pH ranges between 8.1 and 8.2 over most of the shelf. In late spring and summer, following the annual peak in nutrient load, the range of bottom water pH drops below 8.1 over most of the shelf and down to 7.5 in some regions (Figure 2b). Since the production/consumption mechanisms for DIC and O_2 are related (i.e., DIC consumption by

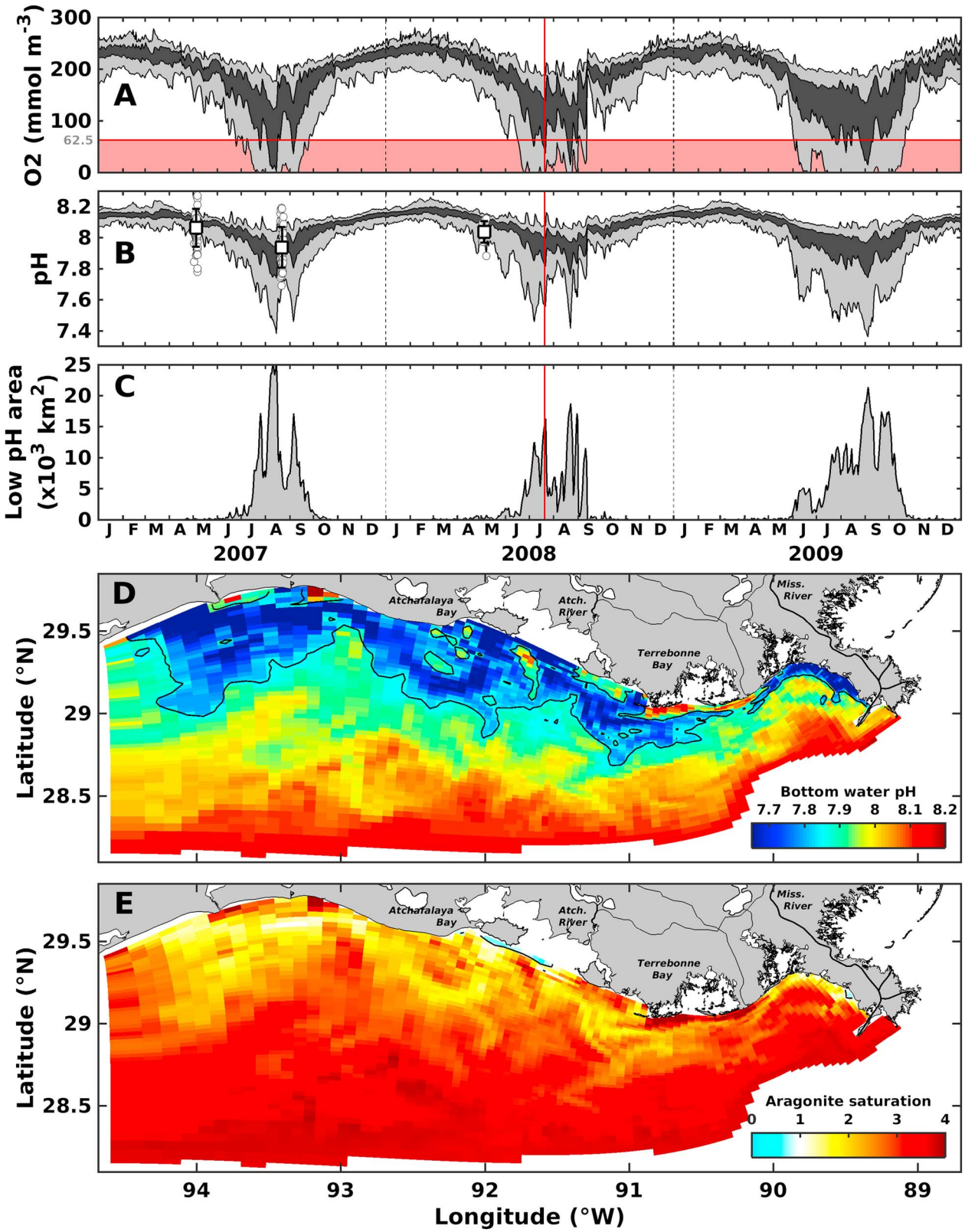

Figure 2. Simulated temporal evolution of bottom water (a) O_2 and (b) pH and of the (c) areal extent of pH < 7.85, and spatial distribution of bottom water (d) pH and (e) aragonite saturation on 21 July 2008. Light and dark grey areas in Figures 2a and 2b indicate the 2.5th–97.5th and 25th–75th percentile ranges, respectively. In Figure 2b bottom water pH observations from *Cai et al.* [2011] are shown as white dots and mean ±1 SD as white squares. In Figures 2d and 2e the black contour lines indicate a pH of 7.85, which we define as the threshold for acidified water, and the aragonite saturation horizon $\Omega_A = 1$, respectively.

Table 1. Comparison Between Simulated and Observed Vertically Integrated DIC Production in the Water Column, DIC Efflux From the Sediment, and Total DIC Production (Water Column + Sediment)[a]

	Water Column					Sediment					Total	
	Model		Observations			Model		Observations			Model	Observations
	Mean	SD	Mean	SD	*N*	Mean	SD	Mean	SD	*N*		
Oct–Apr	31.9	11.5	86.9	60.5	126	8.7	3.4	15.8	4.8	7	40.6	102.7
May–Sep	54.6	5.2	102.7	59.5	386	16.7	3.5	17.6	2.8	9	71.4	120.3
Hypoxic	51.9	15.2	119.0	46.7	63	20.9	4.9	17.1	3.2	6	72.9	136.1

[a]Values are reported in mmol C m^{-2} d^{-1}. Hypoxic refers to time and locations with hypoxic bottom waters. Water column respiration observations are from *Murrell and Lehrter* [2011] and sediment efflux of DIC from *Lehrter et al.* [2012].

primary production and DIC production by respiration in water column and sediment), the time series of average bottom water pH and O_2 are strongly correlated on the shelf ($r = 0.88$, $p < 0.01$). On average, pH is 7.73 (SD = 0.12) in hypoxic bottom waters and 8.08 (SD = 0.08) outside the hypoxic zone. Outside the hypoxic season from June to September, average bottom water pH is 8.12 (SD = 0.06) on the shelf.

For further analysis and discussion, we refer to regions with pH less than or equal to 7.85 as acidified. This value is the average pH observed at the limit between normoxic ($O_2 > 62.5$ mmol O_2 m^{-3}) and hypoxic waters on the shelf [*Cai et al.*, 2011]. Acidified waters are not necessarily undersaturated (i.e., corrosive) with respect to aragonite ($\Omega_A < 1$) due to the high alkalinity in this region [*Wang et al.*, 2013]. At a bottom water pH of 7.85, Ω_A is 2.63 (SD = 0.25). The average Ω_A in acidified bottom water is 2.12 (SD = 0.50). For comparison, Ω_A is 3.51 (SD = 0.37) elsewhere. Acidified bottom waters occur mainly from June to September (Figure 2c) and coincide in time and space with the hypoxic zone, consistent with observations [*Cai et al.*, 2011; *Sunda and Cai*, 2012]. This is not surprising since the mechanisms controlling acidification and hypoxia (stratification and respiration) are the same. Acidified bottom waters occupy, on average, an area of $7.02 \cdot 10^3$ km^2 (SD = $6.01 \cdot 10^3$) in summer (June to September) with a maximum annual extent of $22 \cdot 10^3$ km^2 (2007–2009 average). The maximum extent represents 42% of the shelf area ($z \leq 50$ m) west of the Mississippi River delta in our model (Figures 2c and 2d).

The spatial distributions of simulated bottom pH and Ω_A on 21 July 2008, during a midsummer peak of acidification, are shown in Figures 2d and 2e (a 3 year animation is available in supporting information Movie S1). Other peaks in acidification occur in late August (Figure 2c). During summer peaks of acidification, extensive areas of low pH bottom waters are found in the areas shallower than 20 m (Figure 2d). Similar patterns, with variation in timing and location, are found in 2007 and 2009 (Movie S1b). The aragonite saturation state decreases within the acidified regions but rarely approaches undersaturation ($\Omega_A < 1$; Figure 2e and Movie S1b). The acidified waters are therefore not corrosive with respect to aragonite. Although transient in time, near the Mississippi River delta acidified waters are usually confined to water depths < 20 m (Movie S1). On the western shelf, low pH bottom waters are more spatially heterogeneous than near the Mississippi Delta. This spatial variability is partly driven by differences in stratification between the eastern, strongly stratified and the western, more weakly stratified regions and mirrors the spatial structure of hypoxia [*Hetland and DiMarco*, 2008].

3.2. Mechanisms of Acidification

Simulated and observed values of vertically integrated DIC production in the water column and DIC efflux from the sediment are shown in Table 1. Fluxes are for the entire shelf during the hypoxic season (May to September) and the rest of the year (October to April), and for hypoxic locations only. During the hypoxic season (May to September), total simulated DIC production on the shelf is 71.4 mmol C m^{-2} d^{-1} on average and dominated by water column respiration (76% of total respiration). Total simulated DIC production drops to 40.6 mmol C m^{-2} d^{-1} for the rest of the year; water column respiration represents 79% of total respiration during this period. Within hypoxic locations only, total DIC production is similar to the shelf average with 72.9 mmol C m^{-2} d^{-1} and remains dominated by water column respiration (71% of total respiration). Therefore, DIC production through water column respiration comprises at least two thirds of the total DIC production on the shelf. Overall, simulated water column respiration is lower than the observations, but within one standard deviation (Table 1). Sediment DIC flux agrees well with the observations during the

Table 2. Simulated, Vertically Integrated DIC Production (mmol $m^{-2} d^{-1}$) Due To Various Biological Processes Throughout the Whole Water Column and for the 5 m Thick Bottom Layer, and Alkalinity Sink (mmol $m^{-2} d^{-1}$) Due To Nitrification and NH_4^+ Uptake[a]

	DIC Production								Alkalinity Sink					
	Zooplankton Respiration		Remineralization						Sediment DIC Efflux		Nitrification		NH_4^+ Uptake	
			Small Detritus		Large Detritus		River DOM							
						Water Column								
Oct–Apr	6.7	14%	**20.3**	**42%**	0.3	< 1%	4.7	12%	8.7	18%	3.4	7%	3.4	7%
May–Sep	**19.8**	**24%**	**28.8**	**34%**	0.5	< 1%	5.5	8%	**16.7**	**21%**	4.9	6%	6.2	7%
Hypoxic	**19.8**	**22%**	**26.2**	**29%**	0.3	< 1%	5.5	8%	**20.9**	**29%**	5.0	6%	6.1	6%
						Bottom 5 m								
Oct–Apr	2.1	11%	**5.4**	**27%**	0.1	< 1%	1.6	11%	**8.7**	**42%**	1.1	5%	0.5	3%
May–Sep	4.2	13%	6.1	19%	0.1	< 1%	1.6	7%	**16.7**	**53%**	1.7	5%	0.8	3%
Hypoxic	5.1	12%	7.2	17%	0.1	< 1%	2.7	8%	**20.9**	**55%**	2.7	6%	1.0	2%

[a]Fluxes are averaged for the periods from October to April, from May to September, and for hypoxic locations only. The percentages indicate the contribution of each process to the decrease in pH (see section 2). The dominant contribution for each period/region is given in bold.

hypoxic season (May to September) and within the hypoxic area. For the rest of the year few observations are available and only for April. In August 2007, when the observations by *Cai et al*. [2011] were collected (Figure 1), simulated sediment DIC flux was on average 21.1 ± 4.9 mmol C $m^{-2} d^{-1}$ on the shelf, which compares well with the observations of *Lehrter et al*. [2012] for the same time (17.7 ± 4.2 mmol C $m^{-2} d^{-1}$).

In the model, local decreases in pH result from the addition of DIC and the removal of alkalinity. DIC is added via five distinct processes: zooplankton respiration, microbial remineralization of small and large detritus and of river DOM (all in the water column), and efflux of DIC from the sediment. Alkalinity is removed in the water column through nitrification and NH_4^+ uptake. We now focus our discussion on these processes and their relative importance for lowering pH (DIC and alkalinity fluxes are reported as integrals over the whole water column and integrals over only the bottommost 5 m in Table 2). The simulated DIC production during the hypoxic season accounts for 88% of the decrease in pH throughout the water column, while alkalinity losses due to nitrification and NH_4^+ uptake have a small effect on pH (Table 2). When the whole water column is considered, the remineralization of small detritus accounts for over 40% of the DIC production on the shelf, regardless of the season, and is the largest biological source of DIC. The small detritus pool is distinct from river DOM in the model and represents autochthonous organic matter produced on the shelf. Zooplankton respiration and influx of DIC from the sediment are the second and third largest contributors. Within the region where bottom waters are hypoxic and where acidification is most pronounced, sediment respiration (20.9 mmol C $m^{-2} d^{-1}$) is larger than the shelf-wide averages and contributes as much as small detritus remineralization to the decrease in pH (29%, Table 2). Zooplankton respiration (19.8 mmol C $m^{-2} d^{-1}$) is also an important contributor to DIC production in this region, while the remineralization of large detritus is negligible. *Fichot and Benner* [2014] found a mixed-layer remineralization rate for terrigenous dissolved organic carbon of 4.7 mmol C $m^{-2} d^{-1}$ in summer, which is similar to the simulated shelf average for the remineralization of river DOM (5.5 mmol C $m^{-2} d^{-1}$). While the remineralization of river DOM may affect surface pCO_2 levels [*Fichot and Benner*, 2014], its contribution to bottom acidification is negligible (Table 2).

Integrating fluxes over the whole water column underestimates the relative importance of the sediment influx of CO_2. On the northern Gulf of Mexico shelf, hypoxia is mainly confined to the bottom boundary layer, which typically extends less than 5 m from the bottom [*Wiseman et al*., 1997; *Fennel et al*., 2013, 2016; *Obenour et al*., 2013; *Yu et al*., 2015a]. Since acidification is due to the same processes as hypoxia development, it is reasonable to assume that low pH waters are equally constrained to the bottom boundary layer and this is indeed the case in our model simulation. The average thickness of acidified bottom waters (pH < 7.85) is 2.3 m (SD = 1.9), and 87% of the acidified waters are found within 5 m above the bottom. Considering DIC production in the bottommost 5 m thus gives a better indication of the relative importance of different metabolic processes on acidification. In the bottommost 5 m sediment respiration is the dominant process,

representing on average over half of the total DIC production during the hypoxic season (May to September) and contributing 55% to the decrease of pH in hypoxic bottom waters (Table 2). The remineralization of small detritus and zooplankton respiration contribute only 17% and 12%, respectively (Table 2). These results suggest that the production of DIC by benthic metabolic processes is key to the acidification of bottom waters and are consistent with previous findings that hypoxia generation in this region is driven by sediment oxygen consumption [*Fennel et al*., 2013; *Yu et al*., 2015a].

The strong stratification during summer, which is due to the large freshwater input during the preceding months, is an important driver of bottom water acidification on the shelf and can be considered a prerequisite for eutrophication-induced acidification more generally. In fact, studies in well-mixed coastal systems have found that enhanced biological production can lead to an increase in pH through DIC removal by photosynthesis, resulting in basification rather than acidification [*Borges and Gypens*, 2010; *Flynn et al*., 2015; *Nixon et al*., 2015]. Moreover, within the surface mixed layer, primary production, organic matter respiration, and air-sea CO_2 exchange can counteract each other to some degree thus mitigating any accumulation of DIC. A vertical (or temporal) decoupling between primary production and respiration is a necessary condition for lower pH in bottom waters [*Duarte et al*., 2013].

According to our simulation, river DOM plays a negligible role in acidification. Eutrophication-driven acidification in this region is driven by local biological production, which results from the inorganic river nutrient load and represents the main source of POM deposition on the shelf [*Redalje et al*., 1994; *Justić et al*., 1996; *Rowe and Chapman*, 2002], rather than the remineralization of allochthonous DOM. This is noteworthy because significant terrestrial organic carbon degradation occurs on continental shelves [*Cai*, 2011; *Fichot and Benner*, 2014]. This finding has important implications for nutrient management in the watershed, namely, that reductions of inorganic nutrient loads appear to be the most effective approach to mitigating bottom water acidification and hypoxia in this region.

4. Conclusions

We present the first high-resolution simulation of eutrophication-driven bottom water acidification in the northern Gulf of Mexico. Our model suggests that an extended area of acidified bottom water develops every summer on the shelf, the spatial distribution of which coincides with that of hypoxic waters and agrees well with the observed extent in 2007 when shelf-wide observations are available. For the most part, acidified waters are not corrosive to calcifying organisms ($\Omega_A > 1$). Acidification and hypoxia generation in bottom waters are driven by a combination of microbial respiration of organic matter that is primarily produced locally from riverine inorganic nutrient loads, and strong vertical stratification that results from the significant freshwater inputs. In our model, the largest DIC source in the water column is from the remineralization of suspended detritus. However, our model suggests that in analogy to hypoxic conditions, acidified water is restricted to the bottom boundary layer. When considering the biological fluxes that add DIC to this layer, the sediment is the dominant contributor. The contribution of allochthonous dissolved organic matter is small as a source of DIC in the water column and negligible for bottom water acidification. This implies that acidification as well as hypoxia generation are linked to autochthonous production driven by river nutrients and therefore can be mitigated by management of inorganic nutrients in the watershed.

Acknowledgments
Model outputs used in this publication are available from the authors upon request (arnaud.laurent@dal.ca). All other data are properly cited and referred to in the reference list. This work was supported by NOAA CSCOR grants NA06N0S4780198 and NA09N0S4780208. NGOMEX publication number 214.

References

Altieri, A. H., and K. B. Gedan (2014), Climate change and dead zones, *Global Change Biol.*, 1–12, doi:10.1111/gcb.12754.

Anderson, L. A., and J. L. Sarmiento (1994), Redfield ratios of remineralization determined by nutrient data analysis, *Global Biogeochem. Cycles*, *8*, 65–80, doi:10.1029/93GB03318.

Aulenbach, B., H. Buxton, W. Battaglin, and R. Coupe (2007), Streamflow and nutrient fluxes of the Mississippi-Atchafalaya River basin and subbasins for the period of record through 2005, *Open-File Rep. 2007–1080, U.S. Geol. Surv.*

Borges, A. V., and N. Gypens (2010), Carbonate chemistry in the coastal zone responds more strongly to eutrophication than to ocean acidification, *Limnol. Oceanogr.*, *55*(1), 346–353, doi:10.4319/lo.2010.55.1.0346.

Breitburg, D. L., D. W. Hondorp, L. A. Davias, and R. J. Diaz (2009), Hypoxia, nitrogen, and fisheries: Integrating effects across local and global landscapes, *Annu. Rev. Mar. Sci.*, *1*, 329–349, doi:10.1146/annurev.marine.010908.163754.

Breitburg, D. L., et al. (2015), And on top of all that… Coping with ocean acidification in the midst of many stressors, *Oceanography*, *28*(2), 48–61, doi:10.5670/oceanog.2015.31.

Cai, W.-J. (2011), Estuarine and coastal ocean carbon paradox: CO_2 sinks or sites of terrestrial carbon incineration?, *Annu. Rev. Mar. Sci.*, *3*, 123–145, doi:10.1146/annurev-marine-120709-142723.

Cai, W.-J., X. Hu, W.-J. Huang, L.-Q. Jiang, Y. Wang, T.-H. Peng, and X. Zhang (2010), Alkalinity distribution in the western North Atlantic Ocean margins, *J. Geophys. Res.*, *115*, C08014, doi:10.1029/2009JC005482.

Cai, W.-J., et al. (2011), Acidification of subsurface coastal waters enhanced by eutrophication, *Nat. Geosci.*, *4*(11), 766–770, doi:10.1038/ngeo1297.

Da Silva, A., C. Young, and S. Levitus (1994a), *Atlas of Surface Marine Data 1994, Vol. 3. Anomalies of Heat and Momentum Fluxes, NOAA Atlas NESDIS 8*, U.S. Dept. Commer., Washington, D. C.

Da Silva, A., C. Young, and S. Levitus (1994b), *Atlas of Surface Marine Data 1994, Vol. 4. Anomalies of Heat and Momentum Fluxes, NOAA Atlas NESDIS 8*, U.S. Dept. Commer., Washington, D. C.

Diaz, R. J., and R. Rosenberg (1995), Marine benthic hypoxia: A review of its ecological effects and the behavioural responses of benthic macrofauna, *Oceanogr. Mar. Biol. Annu. Rev.*, *33*, 245–303.

Diaz, R. J., and R. Rosenberg (2008), Spreading dead zones and consequences for marine ecosystems, *Science*, *321*, 926–929, doi:10.1126/science.1156401.

Dickson, A. G., and F. J. Millero (1987), A comparison of the equilibrium constants for the dissociation of carbonic acid in seawater media, *Deep Sea Res. Part A. Oceanogr. Res. Pap.*, *34*(10), 1733–1743, doi:10.1016/0198-0149(87)90021-5.

Doney, S. C. (2010), The growing human footprint on coastal and open-ocean biogeochemistry, *Science*, *328*(5985), 1512–1516, doi:10.1126/science.1185198.

Duarte, C. M., I. E. Hendriks, T. S. Moore, Y. S. Olsen, A. Steckbauer, L. Ramajo, J. Carstensen, J. A. Trotter, and M. McCulloch (2013), Is ocean acidification an open-ocean syndrome?, Understanding anthropogenic impacts on seawater pH, *Estuaries Coasts*, *36*(2), 221–236, doi:10.1007/s12237-013-9594-3.

Environmental Protection Agency (2008), Mississippi River/Gulf of Mexico watershed nutrient task force Gulf hypoxia action plan 2008 for reducing mitigating, and controlling hypoxia in the northern Gulf of Mexico and improving water quality in the Mississippi River Basin, Washington, D. C.

Eppley, R. W. (1972), Temperature and phytoplankton growth in the sea, *Fish. Bull.*, *70*(4), 1063–1085.

Evans, G., and J. S. Parslow (1985), A model of annual plankton cycles, *Deep Sea Res. Part B. Oceanogr. Lit. Rev.*, *32*(9), 759, doi:10.1016/0198-0254(85)92902-4.

Fennel, K., J. Wilkin, J. Levin, J. Moisan, J. O'Reilly, and D. Haidvogel (2006), Nitrogen cycling in the Middle Atlantic Bight: Results from a three-dimensional model and implications for the North Atlantic nitrogen budget, *Global Biogeochem. Cycles*, *20*, GB3007, doi:10.1029/2005GB002456.

Fennel, K., J. Wilkin, M. Previdi, and R. Najjar (2008), Denitrification effects on air-sea CO_2 flux in the coastal ocean: Simulations for the northwest North Atlantic, *Geophys. Res. Lett.*, *35*, L24608, doi:10.1029/2008GL036147.

Fennel, K., R. Hetland, Y. Feng, and S. DiMarco (2011), A coupled physical-biological model of the Northern Gulf of Mexico shelf: Model description, validation and analysis of phytoplankton variability, *Biogeosciences*, *8*(7), 1881–1899, doi:10.5194/bg-8-1881-2011.

Fennel, K., J. Hu, A. Laurent, M. Marta-Almeida, and R. Hetland (2013), Sensitivity of hypoxia predictions for the northern Gulf of Mexico to sediment oxygen consumption and model nesting, *J. Geophys. Res. Ocean.*, *118*, 990–1002, doi:10.1002/jgrc.20077.

Fennel, K., A. Laurent, R. Hetland, D. Justić, D. S. Ko, J. Lehrter, M. Murrell, L. Wang, L. Yu, and W. Zhang (2016), Effects of model physics on hypoxia simulations for the northern Gulf of Mexico: A model intercomparison, *J. Geophys. Res. Ocean.*, *121*, 5731–5750, doi:10.1002/2015JC011577.

Fichot, C. G., and R. Benner (2014), The fate of terrigenous dissolved organic carbon in a river-influenced ocean margin, *Global Biogeochem. Cycles*, *28*, 300–318, doi:10.1002/2013GB004670.

Flynn, K. J., D. R. Clark, A. Mitra, H. Fabian, P. J. Hansen, P. M. Glibert, G. L. Wheeler, D. K. Stoecker, J. C. Blackford, and C. Brownlee (2015), Ocean acidification with (de)eutrophication will alter future phytoplankton growth and succession, *Proc. Biol. Sci.*, *282*(1804), 20,142,604, doi:10.1098/rspb.2014.2604.

García, H. E., and L. I. Gordon (1992), Oxygen solubility in seawater: Better fitting equations, *Limnol. Oceanogr.*, *37*(6), 1307–1312, doi:10.4319/lo.1992.37.6.1307.

Geider, R., H. MacIntyre, and T. Kana (1997), Dynamic model of phytoplankton growth and acclimation: Responses of the balanced growth rate and the chlorophyll *a*:carbon ratio to light, nutrient-limitation and temperature, *Mar. Ecol. Prog. Ser.*, *148*(1–3), 187–200, doi:10.3354/meps148187.

Geider, R. J., H. L. MacIntyre, and T. M. Kana (1996), A dynamic model of photoadaptation in phytoplankton, *Limnol. Oceanogr.*, *41*(1), 1–15, doi:10.4319/lo.1996.41.1.0001.

Haidvogel, D. B., et al. (2008), Ocean forecasting in terrain-following coordinates: Formulation and skill assessment of the Regional Ocean Modeling System, *J. Comput. Phys.*, *227*(7), 3595–3624, doi:10.1016/j.jcp.2007.06.016.

Hetland, R. D., and S. F. DiMarco (2008), How does the character of oxygen demand control the structure of hypoxia on the Texas–Louisiana continental shelf?, *J. Mar. Syst.*, *70*(1–2), 49–62, doi:10.1016/j.jmarsys.2007.03.002.

Hetland, R. D., and S. F. DiMarco (2012), Skill assessment of a hydrodynamic model of circulation over the Texas–Louisiana continental shelf, *Ocean Model.*, *43–44*, 64–76, doi:10.1016/j.ocemod.2011.11.009.

Ho, D. T., C. S. Law, M. J. Smith, P. Schlosser, M. Harvey, and P. Hill (2006), Measurements of air-sea gas exchange at high wind speeds in the Southern Ocean: Implications for global parameterizations, *Geophys. Res. Lett.*, *33*, L16611, doi:10.1029/2006GL026817.

Ho, D. T., R. Wanninkhof, P. Schlosser, D. S. Ullman, D. Hebert, and K. F. Sullivan (2011), Toward a universal relationship between wind speed and gas exchange: Gas transfer velocities measured with 3 He/SF 6 during the Southern Ocean Gas Exchange Experiment, *J. Geophys. Res.*, *116*, C00F04, doi:10.1029/2010JC006854.

Huang, W.-J., W.-J. Cai, Y. Wang, S. E. Lohrenz, and M. C. Murrell (2015), The carbon dioxide system on the Mississippi River-dominated continental shelf in the northern Gulf of Mexico: 1. Distribution and air-sea CO_2 flux, *J. Geophys. Res. Ocean.*, *120*, 1429–1445, doi:10.1002/2014JC010498.

Jahnke, R. A., D. B. Craven, D. C. McCorkle, and C. E. Reimers (1997), $CaCO_3$ dissolution in California continental margin sediments: The influence of organic matter remineralization, *Geochim. Cosmochim. Acta*, *61*(17), 3587–3604, doi:10.1016/S0016-7037(97)00184-1.

Justić, D., and L. Wang (2014), Assessing temporal and spatial variability of hypoxia over the inner Louisiana–upper Texas shelf: Application of an unstructured-grid three-dimensional coupled hydrodynamic-water quality model, *Cont. Shelf Res.*, *72*, 163–179, doi:10.1016/j.csr.2013.08.006.

Justić, D., N. Rabalais, and R. E. Turner (1996), Effects of climate change on hypoxia in coastal waters: A doubled CO_2 scenario for the northern Gulf of Mexico, *Limnol. Oceanogr.*, *41*(5), 992–1003, doi:10.4319/lo.1996.41.5.0992.

Ko, D., R. Gould, B. Penta, and J. Lehrter (2016), Impact of satellite remote sensing data on simulations of coastal circulation and hypoxia on the Louisiana Continental Shelf, *Remote Sens.*, *8*(5), 435, doi:10.3390/rs8050435.

Langseth, B. J., K. M. Purcell, J. K. Craig, A. M. Schueller, J. W. Smith, K. W. Shertzer, S. Creekmore, K. A. Rose, and K. Fennel (2014), Effect of changes in dissolved oxygen concentrations on the spatial dynamics of the Gulf Menhaden fishery in the Northern Gulf of Mexico, *Mar. Coast. Fish.*, *6*(1), 223–234, doi:10.1080/19425120.2014.949017.

Laurent, A., and K. Fennel (2014), Simulated reduction of hypoxia in the northern Gulf of Mexico due to phosphorus limitation, *Elem. Sci. Anthr.*, *2*(1), 22, doi:10.12952/journal.elementa.000022.

Laurent, A., K. Fennel, J. Hu, and R. Hetland (2012), Simulating the effects of phosphorus limitation in the Mississippi and Atchafalaya River plumes, *Biogeosciences*, *9*(11), 4707–4723, doi:10.5194/bg-9-4707-2012.

Laurent, A., K. Fennel, R. Wilson, J. Lehrter, and R. Devereux (2016), Parameterization of biogeochemical sediment–water fluxes using in situ measurements and a diagenetic model, *Biogeosciences*, *13*, 77–94, doi:10.5194/bg-13-77-2016.

Lehrter, J. C., D. L. Beddick, and M. C. Murrell (2012), Sediment-water fluxes of dissolved inorganic carbon, O_2, nutrients, and N_2 from the hypoxic region of the Louisiana continental shelf, *Biogeochemistry*, *109*, 233–252, doi:10.1007/s10533-011-9623-x.

Levin, L. A., et al. (2015), Comparative biogeochemistry–ecosystem–human interactions on dynamic continental margins, *J. Mar. Syst.*, *141*, 3–17, doi:10.1016/j.jmarsys.2014.04.016.

Lohrenz, S. E., M. J. Dagg, and T. E. Whitledge (1990), Enhanced primary production at the plume/oceanic interface of the Mississippi River, *Cont. Shelf Res.*, *10*(7), 639–664.

Lohrenz, S. E., G. L. Fahnenstiel, D. G. Redalje, G. A. Lang, M. J. Dagg, T. E. Whitledge, and Q. Dortch (1999), Nutrients, irradiance, and mixing as factors regulating primary production in coastal waters impacted by the Mississippi River plume, *Cont. Shelf Res.*, *19*(9), 1113–1141, doi:10.1016/S0278-4343(99)00012-6.

Marta-Almeida, M., R. D. Hetland, and X. Zhang (2013), Evaluation of model nesting performance on the Texas-Louisiana continental shelf, *J. Geophys. Res. Ocean.*, *118*, 1–16, doi:10.1002/jgrc.20163.

Mattern, J. P., K. Fennel, and M. Dowd (2013), Sensitivity and uncertainty analysis of model hypoxia estimates for the Texas-Louisiana shelf, *J. Geophys. Res. Ocean.*, *118*, 1316–1332, doi:10.1002/jgrc.20130.

Mehrbach, C., C. H. Culberson, J. E. Hawley, and R. M. Pytkowicz (1973), Measurement of the apparent dissociation constants of carbonic acid in seawater at atmospheric pressure, *Limnol. Oceanogr.*, *18*(6), 897–907, doi:10.4319/lo.1973.18.6.0897.

Mesinger, F., et al. (2006), North American regional reanalysis, *Bull. Am. Meteorol. Soc.*, *87*(3), 343–360, doi:10.1175/BAMS-87-3-343.

Morse, J. W., and P. M. Eldridge (2007), A non-steady state diagenetic model for changes in sediment biogeochemistry in response to seasonally hypoxic/anoxic conditions in the "dead zone" of the Louisiana shelf, *Mar. Chem.*, *106*(1–2), 239–255, doi:10.1016/j.marchem.2006.02.003.

Murrell, M. C., and J. C. Lehrter (2011), Sediment and lower water column oxygen consumption in the seasonally hypoxic region of the Louisiana Continental Shelf, *Estuaries Coasts*, *34*(5), 912–924, doi:10.1007/s12237-010-9351-9.

Nixon, S. W., A. J. Oczkowski, M. E. Q. Pilson, L. Fields, C. A. Oviatt, and C. W. Hunt (2015), On the response of pH to inorganic nutrient enrichment in well-mixed coastal marine waters, *Estuaries Coasts*, *38*(1), 232–241, doi:10.1007/s12237-014-9805-6.

Obenour, D. R., D. Scavia, N. N. Rabalais, R. E. Turner, and A. M. Michalak (2013), Retrospective analysis of midsummer hypoxic area and volume in the Northern Gulf of Mexico, 1985–2011, *Environ. Sci. Technol.*, *47*(17), 9808–9815, doi:10.1021/es400983g.

Paerl, H. W. (2006), Assessing and managing nutrient-enhanced eutrophication in estuarine and coastal waters: Interactive effects of human and climatic perturbations, *Ecol. Eng.*, *26*(1), 40–54, doi:10.1016/j.ecoleng.2005.09.006.

Rabalais, N. N., R. E. Turner, Q. Dortch, D. Justić, V. Bierman, and W. Wiseman (2002a), Nutrient-enhanced productivity in the northern Gulf of Mexico: Past, present and future, *Hydrobiologia*, *475–476*(1), 39–63, doi:10.1023/A:1020388503274.

Rabalais, N. N., R. E. Turner, and D. Scavia (2002b), Beyond science into policy: Gulf of Mexico hypoxia and the Mississippi River, *BioScience*, *52*(2), 129, doi:10.1641/0006-3568(2002)052[0129:BSIPGO]2.0.CO;2.

Rabalais, N. N., R. E. Turner, B. K. Sen Gupta, D. F. Boesch, P. Chapman, and M. C. Murrell (2007), Hypoxia in the Northern Gulf of Mexico: Does the science support the plan to reduce, mitigate, and control hypoxia?, *Estuaries Coasts*, *30*(5), 753–772, doi:10.1007/BF02841332.

Rabouille, C., F. T. Mackenzie, and L. M. Ver (2001), Influence of the human perturbation on carbon, nitrogen, and oxygen biogeochemical cycles in the global coastal ocean, *Geochim. Cosmochim. Acta*, *65*(21), 3615–3641, doi:10.1016/S0016-7037(01)00760-8.

Rabouille, C., et al. (2008), Comparison of hypoxia among four river-dominated ocean margins: The Changjiang (Yangtze), Mississippi, Pearl, and Rhône rivers, *Cont. Shelf Res.*, *28*(12), 1527–1537, doi:10.1016/j.csr.2008.01.020.

Redalje, D. G., S. E. Lohrenz, and G. L. Fahnenstiel (1994), The relationship between primary production and the vertical export of particulate organic matter in a river-impacted coastal ecosystem, *Estuaries*, *17*(4), 829, doi:10.2307/1352751.

Ren, W., H. Tian, B. Tao, J. Yang, S. Pan, W. Cai, S. E. Lohrenz, R. He, and C. S. Hopkinson (2015), Large increase in dissolved inorganic carbon flux from the Mississippi River to Gulf of Mexico due to climatic and anthropogenic changes over the 21st century, *J. Geophys. Res. Biogeosciences*, *120*, 1–13, doi:10.1002/2014JG002761.

Rose, K. A., et al. (2009), Does hypoxia have population-level effects on coastal fish?, Musings from the virtual world, *J. Exp. Mar. Bio. Ecol.*, *381*, S188–S203, doi:10.1016/j.jembe.2009.07.022.

Rowe, G. T., and P. Chapman (2002), Continental shelf hypoxia: Some nagging questions, *Gulf Mex. Sci.*, *2*, 155–160.

Schaeffer, B. A., G. A. Sinclair, J. C. Lehrter, M. C. Murrell, J. C. Kurtz, R. W. Gould, and D. F. Yates (2011), An analysis of diffuse light attenuation in the northern Gulf of Mexico hypoxic zone using the SeaWiFS satellite data record, *Remote Sens. Environ.*, *115*(12), 3748–3757, doi:10.1016/j.rse.2011.09.013.

Selberg, C. D., L. A. Eby, and L. B. Crowder (2001), Hypoxia in the Neuse River Estuary: Responses of blue crabs and crabbers, *North Am. J. Fish. Manag.*, *21*(2), 358–366, doi:10.1577/1548-8675(2001)021<0358:HITNRE>2.0.CO;2.

Soetaert, K., P. M. J. Herman, and J. J. Middelburg (1996a), A model of early diagenetic processes from the shelf to abyssal depths, *Geochim. Cosmochim. Acta*, *60*(6), 1019–1040, doi:10.1016/0016-7037(96)00013-0.

Soetaert, K., P. M. J. Herman, J. J. Middelburg, C. Heip, H. S. DeStigter, T. C. E. van Weering, E. Epping, and W. Helder (1996b), Modeling 210Pb-derived mixing activity in ocean margin sediments: Diffusive versus nonlocal mixing, *J. Mar. Res.*, *54*, 1207–1227, doi:10.1357/0022240963213808.

Sunda, W. G., and W.-J. Cai (2012), Eutrophication induced CO_2-acidification of subsurface coastal waters: Interactive effects of temperature, salinity, and atmospheric PCO_2, *Environ. Sci. Technol.*, *46*(19), 10,651–10,659, doi:10.1021/es300626f.

Wang, Z. A., R. Wanninkhof, W.-J. Cai, R. H. Byrne, X. Hu, T.-H. Peng, and W.-J. Huang (2013), The marine inorganic carbon system along the Gulf of Mexico and Atlantic coasts of the United States: Insights from a transregional coastal carbon study, *Limnol. Oceanogr.*, *58*(1), 325–342, doi:10.4319/lo.2013.58.1.0325.

Wanninkhof, R. (2014), Relationship between wind speed and gas exchange over the ocean revisited, *Limnol. Oceanogr. Methods*, *12*(6), 351–362, doi:10.4319/lom.2014.12.351.

Wiseman, W. J., N. N. Rabalais, R. E. Turner, S. P. Dinnel, and A. MacNaughton (1997), Seasonal and interannual variability within the Louisiana coastal current: Stratification and hypoxia, *J. Mar. Syst.*, *12*, 237–248, doi:10.1016/S0924-7963(96)00100-5.

Wolf-Gladrow, D. A., R. E. Zeebe, C. Klaas, A. Körtzinger, and A. G. Dickson (2007), Total alkalinity: The explicit conservative expression and its application to biogeochemical processes, *Mar. Chem.*, *106*(1–2), 287–300, doi:10.1016/j.marchem.2007.01.006.

Yu, L., K. Fennel, and A. Laurent (2015a), A modeling study of physical controls on hypoxia generation in the northern Gulf of Mexico, *J. Geophys. Res. Ocean.*, *120*, 5019–5039, doi:10.1002/2014JC010634.

Yu, L., K. Fennel, A. Laurent, M. C. Murrell, and J. C. Lehrter (2015b), Numerical analysis of the primary processes controlling oxygen dynamics on the Louisiana shelf, *Biogeosciences*, *12*(7), 2063–2076, doi:10.5194/bg-12-2063-2015.